Effect of Price Responsive Demand on the Operation of Microgrids

Felipe Ramos
University of Waterloo
Waterloo, Canada
frg@conecta.cl

Claudio Cañizares
University of Waterloo
Waterloo, Canada
ccanizar@uwaterloo.ca

Kankar Bhattacharya
University of Waterloo
Waterloo, Canada
kankar@uwaterloo.ca

***Abstract*—In this paper, a demand elasticity model is developed and tested for the dispatch of microgrids. The price obtained from dispatching the network in a base-case scenario is used as input to a demand elasticity model; this demand model is then used to determine the price-responsive demand for the next iteration, assuming that the load schedule is defined a day ahead. Using this scheme, trends for demand, hourly prices, and total operation costs for a microgrid can be obtained, to study the impact of demand response on unit commitment. This way, for a microgrid, the effect on the scheduling of diesel generators and energy storage systems can be analyzed with respect to price-elastic loads. The results for a benchmark microgrid show that the proposed 24-hour model eventually converges to a steady state, with prices and costs at their lowest values for different scenarios. Moreover, it is confirmed that elastic demand in a microgrid reduces electricity price variability and mitigates the need for storage in the presence of high penetration of renewable energy.**

***Keywords*—Microgrid dispatch, demand response, DSM, energy storage, demand elasticity, optimization.**

Nomenclature

Indexes

d	Directly controllable loads.
g	Generator unit.
i, j	System buses.
s	Storage devices.
t, k	Time steps.

Variables

$\delta_{i,t}$	Voltage angle at bus i, time t [rad].
$P_{DC\,d,t}$	Energy curtailed or shifted of load d at time t [kWh].
$P_{DS\,d,t}$	Energy shifted of load d to time t [kWh].
$P_{G\,g,t}$	Energy generated by unit g at time t [kWh].
$P_{S\,s,t}$	Energy absorbed or delivered by storage device s at time t [kWh].
$\rho_{i,t}$	Electricity price at bus i, time t [\$/kWh].
$SOC_{s,t}$	State of charge at storage device s, time t [kW].
$U_{G\,g,t}$	Start-up decision for unit g at time t.
$V_{G\,g,t}$	Shutdown decision for unit g at time t.
$W_{sc\,s,t}$	Binary decision on charging s at time t.
$W_{sd\,s,t}$	Binary decision on discharge s at time t.
$W_{D\,d,t}$	Binary curtailment decision of d at time t.
$W_{G\,g,t}$	ON/OFF status of generator g at time t.

Parameters

a_g	Fixed cost of generator g [\$].
α_i	Share of elastic demand from total demand at bus i [%].
$B_{i,j}$	Susceptance of line i and j [pu].
b_g	Variable cost of generator g [\$/kWh].
C_s^{min}, C_s^{max}	Minimum and maximum storage s charge level [kWh].
C_d	Cost of controllable load d [\$/kWh].
C_s	Cost of storage per operation [\$].
E_i	Crossed-time elasticity matrix at bus i.
$\varepsilon_{it,k}$	Elasticity element t, k of matrix E_i.
η_s^c	Input efficiency of storage device s [%].
η_s^d	Output efficiency of storage device s [%].
G_g	Time for which g must be ON at start to satisfy MUT_g.
L_g	Time for which g must be OFF at start to satisfy MDT_g.
M_s	Constant for enforcing binding conditions on s.
MDT_g, MUT_g	Minimum down and up time of unit g.
$P_{0_{i,t}}$	Initial demand at bus i [kW].
$P_{DG\,i,t}$	Renewable energy injected at bus i at time t [kWh].
$P_{D_d}^{max}$	Maximum power shifted or curtailed for load d [kW].
$P_{D\,i,t}$	Demand at bus i at time t [kWh].
$P_{G_g}^{min}, P_{G_g}^{max}$	Minimum and maximum power limits of generator g [kW].
$P_{i,j}^{line}$	Limit of the line between i and j [kW].
$P_{S_s}^{min}, P_{S_s}^{max}$	Minimum and maximum capability of converter s [kW].

This work was funded by the NSERC Strategic Network on Smart Microgrids (NSMG-Net), Canada.

Paper submitted to Power Systems Computation Conference, August 18-22, 2014, Wroclaw, Poland, organized by Power Systems Computation Conference and Wroclaw University of Technology.

$Ramp_g^{down}$	Ramp down limit of g [kW].
$Ramp_g^{up}$	Ramp up limit of g [kW].
ρ_{i0}	Reference electricity price at bus i [$/kWh].
SDC_g	Shutdown cost of generator g [$].
SUC_g	Start-up cost of generator g [$].
W_{0g}	Status of generator g at t=0.

I. Introduction

With the evolution of smart grids and distributed energy resources (DER), the concept of demand response (DR) has gained more significance. It is expected that appliances and loads in general would have the capability of reacting to external signals, such as prices and direct scheduling commands. DR would also provide various system support services such as operational reserves, frequency response, and/or congestion management [1].

Most of the practical DR examples are associated with programs established by government or utilities, which seek to reduce peak loads or rearrange demand profiles. In the case of voluntary programs, customers may receive a financial incentive by adhering to a program and modifying their demand profiles. Similarly, time-based rates try to sway energy consumption toward a point of mutual convenience for both customers and utilities. This is achieved by offering lower electricity prices at low demand periods, while charging higher prices when the system is stressed or more expensive generating units are in operation.

DR programs may be classified as indirect or direct, depending on whether demand alteration is a choice of customers or a utility decision, respectively. An example of indirect DR is the time-of-use (TOU) pricing scheme [2], which encourages load shifting and curtailment by means of different price levels during the day. Another indirect program is the real-time-pricing (RTP) scheme, which represents the actual short-term conditions of the system [3], thus promoting price-responsive behavior from the customers. Among the direct programs worth mentioning are the direct load control (DLC) and the interruptible load management programs, which pay an incentive to customers [4], allowing the utility to directly control a portion of the load.

One of the most important aspects of assessing the effects of demand responsiveness is how to model both DR and the system. In [5], an elasticity of electricity data collection is presented, classifying between short and long term elasticities, and proving real values estimated for residential and industrial demand price elasticity from different published studies. A statistical method for estimating customers response to pricing signals is developed in [6], which is then used for calculating an optimal RTP scheme that improves the social welfare; from this work, a parallel between DLC programs and instantaneous demand elasticity effects can be derived. In [7], a data mining method is proposed to study responsiveness and create a demand control scheme via pricing signals to control residential heating system devices; a real case study applies the control scheme, reducing peak consumption in up to 11%.

DR studies for an isolated system with renewable energy sources (RES) are conducted in [8] by using two approaches for load shifting, i.e., direct control and customers demand elasticity, showing that with DR less units are committed due to a lower impact of wind variations, thus reducing costs. The work in [9] shows how oligopoly market efficiency is increased when its demand is elastic, noticing that there is reduction in the surplus of producers and consumers. A study of the effects of elasticity from the planning perspective considering operational constraints is conducted in [10] and, by including DR in the short-term optimization models, the work concludes that more RES can be connected with more responsive demand. A unit commitment (UC) method with DR is proposed in [11], which studies economic and environmental impacts, analyzing different DR programs and DLC in order to create a DR program priority list for independent system operators.

So far, most of the work that has been done regarding DR analysis only examines it in an ex-post basis, not properly considering the side effects of intelligent devices and central controllers. In addition, only a few studies consider DERs, DLC, and ESS, all common components to be found in a microgrid. Moreover, the studies performed so far only apply the responsiveness to one day ahead, not taking into account the fact that sustained responsiveness may produce an evolutionary response in demand. This results in a method that is not accurate for estimating the applications and effects of DR in smart grids and microgrids. Therefore, the methodology proposed in this work intends to characterize the possible effects that DR may have over a microgrid. To this end, a 24-hour cross-time elasticity model is developed, based on the behavior that load energy management systems (EMS), such as [12], would have over the networks. Thus, a simplified version of the full extent residential model in [12] is used to obtain a 24-hour elastic model with cross time dependence. This representation of EMS allows for a suitable analysis of the impact of such load control systems on the grid/microgrid.

In order to develop a simulation platform for the study of DR effect on dispatch and vice versa, the mixed integer linear model from [13] is used as a base to develop a model suitable for microgrids. Along with the aforementioned UC model, ESS and DLC are included in the proposed smart-microgrid model. RES in this model are just considered as a negative load component added to the energy balance equation.

The rest of the paper is structured as follows: Demand price-responsiveness and a security-constrained UC model suitable for microgrids are discussed in Section II, together with a proposed procedure for studying demand responsiveness in microgrids. A novel method for estimating demand elasticity parametrization is presented in Section III. In Section IV, a benchmark microgrid and the results of applying the proposed models to this system are presented and discussed. Finally, Section V highlights the most important conclusions and proposes some future work regarding price responsiveness studies in microgrids.

II. Mathematical Modeling

A. Price Elasticity of Demand

The following cross-time elasticity matrix E_i is proposed in [14] and it is used in this work to represent load DR:

$$E_i = \begin{bmatrix} \varepsilon_{i1,1} & \cdots & \varepsilon_{i1,24} \\ \vdots & \ddots & \vdots \\ \varepsilon_{i24,1} & \cdots & \varepsilon_{i24,24} \end{bmatrix} \quad (1)$$

The diagonal elements of E_i, given by $\varepsilon_{it,t}$, represent self-elasticity, i.e., the load i elasticity at time t with respect to price changes at time t. Similarly, non-diagonal elements $\varepsilon_{it,k}$ represent the elasticity of load i at time t with respect to price variations at time k. Note that $\varepsilon_{it,k}$ and $\varepsilon_{k,t}$ do not represent the same, therefore they are not required to have the same value.

The general expression proposed here for estimating demand based on (1) is:

$$P_{Di,t} = P_{0i,t}\left(1 + \alpha_i \sum_k \varepsilon_{it,k}\left(\frac{\rho_{i,k}}{\rho_{i0}} - 1\right)\right) \quad (2)$$

This equation describes demand as a combination of elastic and inelastic demand. Responsiveness is modeled by the total contribution of percentage changes in prices throughout the whole period, which is then multiplied by the base load and its percentage modifier α_i. It is important to note that the result of this elastic term can be positive, zero, or negative, as it represents the total contribution from all price variations for the demand at time t.

In order to properly represent DR, diagonal elements $\varepsilon_{it,t}$ are positive, while non-diagonal elements $\varepsilon_{it,k}$ are negative or zero. In this way, demand variation at hour t is inversely proportional to price variation at t, meaning that a price higher than expected at t would translate into demand reduction at that hour. On the other hand, demand variation at t caused by price variation at k may only be positive when the price difference at time k is not negative. The latter reflects that at a price exceeding the reference ρ_{i0} at time k would encourage an increment of consumption at any other hour, in order to reduce the demand at k (load shifting). In Section III, the estimation of the elasticity parameters to represent load EMS is discussed in some detail.

B. Operational Model for Microgrids

The objective function for the problem is the minimization of the total cost of operation as follows:

$$Cost = \sum_{g,t}\left(a_g W_{Gg,t} + b_g P_{Gg,t} + SUC_g U_{Gg,t} + SDC_g V_{Gg,t}\right) + \\ + \sum_{s,t} C_s\left(W_{scs,t} + W_{sds,t}\right) + \sum_{d,t} C_d P_{DCd,t} \quad (3)$$

The first term in (3) denotes the operational cost of dispatchable generators, including fixed cost when dispatched, variable cost of power output, and startup and shutdown costs. The second term in this equation represents the costs of operating an ESS, while the last term represents the costs of using DLC programs on customers' loads.

1) Demand Supply Balance: The nodal energy balance in the system, including all the distributed components in the microgrid, is represented by:

$$P_{DGi,t} - P_{Di,t} + \sum_{s\in i} P_{S\,s,t} + \sum_{d\in i}\left(P_{DC\,d,t} - P_{DS\,d,t}\right) + \\ + \sum_{g\in i} P_{Gg,t} = \sum_j B_{i,j}\left(\delta_{j,t} - \delta_{i,t}\right) \quad (4)$$

RES in this model are represented as no cost negative loads.

2) Feeder Limit Constraint: The power transferred from bus i to j is constrained by line limits, which is given by:

$$B_{i,j}\left(\delta_{i,t} - \delta_{j,t}\right) \le P_{i,j}^{line} \quad (5)$$

3) Power Generation Limits: For dispatchable generators, the upper and lower operation limits are given as follows:

$$W_{Gg,t} P_{Gg}^{min} \le P_{Gg,t} \le W_{Gg,t} P_{Gg}^{max} \quad (6)$$

4) Startup and Shutdown Coordination: The link between startup and shutdown decisions, and the transition in generator states from one hour to the next one are given by:

$$U_{Gg,t} - V_{Gg,t} = W_{Gg,t} - W_{Gg,t-1} \quad (7)$$

5) Spinning Reserve: For regulation purposes, 10% spinning reserves are assumed as follows:

$$1.10 \sum_i P_{Di,t} \le \sum_g\left(W_{Gg,t} P_{Gg}^{max}\right) \quad (8)$$

6) Ramp Up and Ramp Down Constraints: These constraints ensure that the inter-hour changes for the dispatchable units satisfy necessary ramping limits.

$$P_{Gg,t} - P_{Gg,t-1} \le Ramp_g^{up} \quad (9a)$$

$$P_{Gg,t-1} - P_{Gg,t} \le Ramp_g^{down} \quad (9b)$$

7) Minimum Up and Down Time: The following set of equations account for the minimum up time of dispatchable generators.

$$\sum_{k=1}^{G_g}\left(1 - W_{Gg,k}\right) = 0 \quad (10a)$$

$$\sum_{k=t}^{t+MUT_g-1} W_{Gg,k} \ge MUT_g\left(W_{Gg,t} - W_{Gg,t-1}\right) \\ \forall t = G_g + 1, \ldots, 25 - MUT_g \quad (10b)$$

$$\sum_{k=t}^{24}\left(\left(W_{Gg,t} - W_{Gg,t-1}\right) - W_{Gg,k}\right) \le 0 \\ \forall t = 26 - MUT_g, \ldots, 24 \quad (10c)$$

In (10a), the down time condition for the first G_g time steps is enforced, preventing the generator from shutting down if it was ON during the last steps of the previous iteration. Equation (10b) forces the generator g to be ON at least MUT_g steps if it is switched on. Finally, (10c) provides the condition that

ensures that if a generator is started up within the last MUT_g time steps, it will stay ON until the end of the optimization time frame.

Analogously to the expressions (10a)-(10c), minimum down times are described by the following expressions:

$$\sum_{k=1}^{L_g} W_{Gg,k} = 0 \tag{11a}$$

$$\sum_{k=t}^{t+MDT_g-1} \left(W_{Gg,k} - 1\right) \leq MDT_g \left(W_{Gg,t} - W_{Gg,t-1}\right) \quad \forall t = L_g + 1, \ldots, 25 - MDT_g \tag{11b}$$

$$\sum_{k=t}^{24} \left(W_{Gg,k} - 1 + \left(W_{Gg,t-1} - W_{Gg,t}\right)\right) \leq 0 \quad \forall t = 26 - MDT_g, \ldots, 24 \tag{11c}$$

Equation (11a) enforces the down time condition for the first L_g time steps, preventing the generator from starting if it was OFF at $k = 0$. Equation (11b) forces the generator g to be OFF at least MDT_g steps, and (10c) ensures that if a generator is shutdown within the final MDT_g steps, it will stay OFF until the last period.

8) Energy Storage Systems: The equations to represent ESS in the model are the following:

$$C_s^{min} \leq SOC_{s,t} \leq C_s^{max} \tag{12}$$

$$-P_{S\,s,t}\,\eta_s^c - M_s\,W_{sd\,s,t} \leq SOC_{s,t+1} - SOC_{s,t} \tag{13a}$$

$$SOC_{s,t+1} - SOC_{s,t} \leq -P_{S\,s,t}\,\eta_s^c + M_s\,W_{sd\,s,t} \tag{13b}$$

$$-\frac{P_{S\,s,t}}{\eta_s^d} - M_s\left(W_{sc\,s,t} - W_{sd\,s,t} + 1\right) \leq SOC_{s,t+1} - SOC_{s,t} \tag{14a}$$

$$SOC_{s,t+1} - SOC_{s,t} \leq -\frac{P_{S\,s,t}}{\eta_s^d} + M_s\left(W_{sc\,s,t} - W_{sd\,s,t} + 1\right) \tag{14b}$$

Here, (12) represents the limits in storage capacity level $SOC_{s,t}$ based on the model shown in [15]. Expressions (13a) and (13b) represent the energy balance of the storage device while charging, considering the charging efficiency η_s^c. Equations (14a) and (14b) take care of the discharging process, also considering the operation efficiency η_s^d. It is important to notice that, in order to keep the model linear, the balance equations have been linearized by using the "big" M method for alternative sets of constraints [16], and thus the binding constraints are selected accordingly.

The minimum and maximum capability of ESS energy injection or absorption is modeled as:

$$P_{S\,s}^{\,min} \leq P_{S\,s,t} \leq P_{S\,s}^{\,max} \tag{15}$$

The charging and discharging limits considering the battery SOC and the maximum and minimum storage capacity are modeled as:

$$\frac{\left(SOC_{s,t} - C_s^{max}\right)}{\eta_s^c} \leq P_{S\,s,t} \tag{16a}$$

$$P_{S\,s,t} \leq \left(SOC_{s,t} - C^{min}{}_s\right)\eta_s^d \tag{16b}$$

Finally, coordination of charge/discharge decision variables is achieved by,

$$W_{sd\,s,t} + W_{sc\,s,t} \leq 1 \tag{17}$$

which considers that the ESS cannot charge and discharge at the same time.

9) Direct Controllable Loads: Utility controllable loads are modeled as follows,

$$Type_d \sum_t P_{DC\,d,t} = \sum_t P_{DS\,d,t} \tag{18}$$

$$P_{DC\,d,t} \leq W_{Dd,t}\,P_{D_d}^{max} \tag{19a}$$

$$P_{DS\,d,t} \leq \left(1 - W_{Dd,t}\right)\,P_{D_d}^{max} \tag{19b}$$

where (18) represents the two types of controllable loads: $Type_d = 1$ for shiftable loads, and $Type_d = 0$ for curtailable loads. This equation allows to synthesize both classes of DLC, and is a variation from the constant energy model proposed in [17]; in the case of load shifting, this guarantees that demand that is to be curtailed is reallocated to times where no curtailment is needed. Expressions (19a) and (19b) limit the amount of energy directly controlled, depending on whether the load shed command $W_{Dd,t}$ is in place or not.

With all these equations, the traditional security constraint UC model is modified to represent a microgrid appropriately. In the next section, a general iterative procedure for studying the inter-relationship between price and demand responsiveness is presented, along with the proposed methodology for estimating indirect DR from smart loads.

C. Iterative Procedure

In contrast to what the literature proposes, it is not absolutely correct to assume that demand responsiveness only affects the final demand once. As DR is applied to consecutive days, smart devices or sensitive customers will learn from past behaviors and adapt to the prices resulting from their responsiveness. This changes the procedure to a more iterative one that takes into account this two-way influence between demand and price. Thus, as shown in Fig. 1, the operation of the proposed model is to obtain nodal prices from system simulation, starting with the original values or the forecast for system demand. Then, by using these price vector as the input for a demand elasticity model, the demand for the next iteration is obtained.

III. Load Model Estimation

The value of the expected price ρ_{i0} in (2) is assumed to be constant during the whole time frame (24 hours in this case), as in [10]. By making this assumption, it is ensured that if the prices were all the same, there would be no price

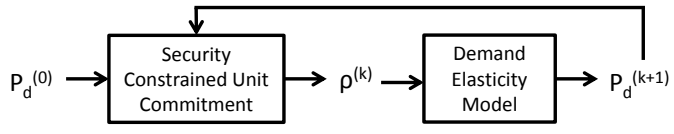

Fig. 1. Iterative procedure for dispatch and demand correction.

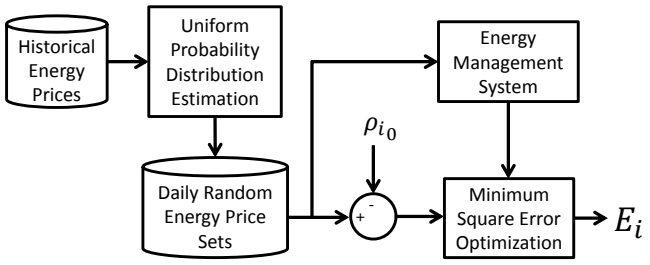

Fig. 2. Demand elasticity model estimation.

variations, translating into no demand variations. Additionally, the expected price should be such that sways demand profiles towards a constant value, agreeing with [7], where the control objective is to reach a flat demand profile. In order to consider these two assumptions, the final value for expected customer price in (2) should be defined by the weighted average of prices at each node, as shown below:

$$\rho_{0_i} = \frac{\sum_t P_{Di,t}\rho_{i,t}}{\sum_t P_{Di,t}} \tag{20}$$

For modeling DR measures, it has been mentioned in the literature that the main components that are represented in DR are water heaters as well as air conditioning, heat and ventilation. However, the proposed model can be extended for more complex demand control devices. Thus, after implementing a model of the load EMS, its response based on the historical data for RTP prices in a certain grid can be assessed. Uniform probability distributions for prices at each hour were considered to determine the impact of varying prices on such load demands; the ranges of these distributions are such that comprises the maximum and minimum prices at each hour, after eliminating the outliers. Once the distribution is parametrized, several daily price sets (24 hour price vectors) are generated and recorded; for each of these vectors, the behavior of the load is obtained. Finally, in the data generation step, each price is compared to the reference price ρ_{i0}, and each demand vector is compared to the base load; in this manner, a set of changes in prices and their corresponding demand variation are created.

After the aforementioned data generation processes, the parameters for the E_i matrix are obtained. A minimum squared error optimization model is used for estimating these parameters based on the difference between the estimated demand from (2) and the actual demand of the loads with EMS. This minimization is subjected to the fact that diagonal elements of matrix E_i are expected to be negative while the rest are positive, properly characterizing DR as explained in Section I. The procedure is illustrated in Fig. 2.

IV. Simulation and Results

A. Test Microgrid Description

The test microgrid used for the studies is a modified version of the CIGRE-IEEE distributed energy sources MV benchmark network proposed in [18]. In this work, the modified system is a 13-bus network, by joining together Buses 0, 1 and 12 in the original system, and replacing the HVDC link with an

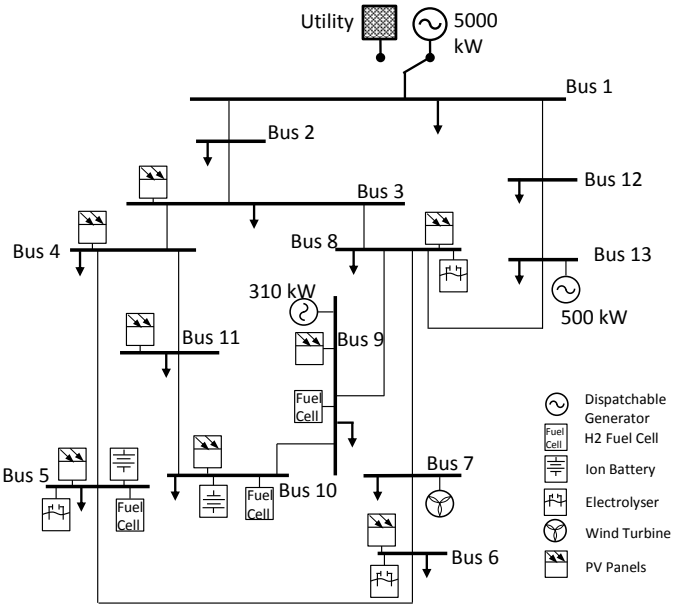

Fig. 3. Microgrid test system based on the CIGRE-IEEE DER benchmark MV network [18].

AC feeder as seen in Fig. 3. The modified microgrid considers 1,710 kW of renewable DERs, 1,339 kWh of ESS installed capacity, and 5,810 kW in dispatchable thermal capacity.

Among the dispatchable thermal generation, the generator at Bus 1 is assumed to be the main microgrid source. The quadratic cost of this large generator (5,000 kW) is here modeled as a 5 step piece-wise linear generator in order to maintain the model linear.

In terms of direct controllable loads, a value corresponding to 7% of the lowest hourly demand for each bus is assumed to be available for curtailment, and 15% for shifting, at any time at each of the load buses. These values were chosen so that only a small percentage of the load is assumed to be controllable, in order to consider a realistic scenario. Since DLC has a major impact on the customers' comfort, the cost of load shifting is assumed to be \$2/kWh, whereas curtailment cost is assumed to be \$20/kWh, which compared to the marginal prices for the microgrid without DR, these costs are about 8 times and 80 times higher, respectively. In this fashion, direct control only occurs when the microgrid load cannot be supplied from the given sources without load reduction.

Finally, the cost C_s of operating the ESS was estimated by considering 2 operating cycles per day, an annual rate of return of 8%, an investment cost of \$1,200/kWh, and a lifespan of 3,000 cycles, as per [19]. Using these values for calculating a daily annuity, the resulting average ESS operating cost is 54¢/kWh.

B. Elasticity Estimation Results

After applying the procedure indicated in Section III for RTP values in Ontario, Canada, during summer, the resulting E_i matrix for the EMS proposed in [12] is shown in Table

TABLE I. DEMAND ELASTICITY MATRIX ESTIMATED FOR THE LOAD EMS IN [12].

	1	2	3	4	5	6	7	8	9	10	11	12	13	14	15	16	17	18	19	20	21	22	23	24
1	**-0.9**	0.3	0.4	0.1		0.0	0.1		0.0	0.1	0.1	0.1				0.1								
2	0.7	**-8.9**	1.1	2.0		0.8	0.5	0.1		1.1	0.2	0.7	0.6		1.0	0.9		0.2	0.1	0.1				
3	0.3	1.2	**-3.7**	0.8	0.7	0.0	0.1	0.2								0.3		0.3			0.1		0.2	
4	0.1	0.7	0.8	**-3.7**	0.5	0.1	0.1					0.4		0.6		0.1			0.1	0.1	0.1	0.1		
5		0.0	0.2	0.3	**-2.6**	0.3	0.1		0.1	0.1	0.3	0.0	0.2	0.0		0.2	0.3	0.1	0.0			0.0		
6		0.3	0.1		0.1	**-2.2**	0.1		0.0			0.0	0.2	0.1	0.3	0.3	0.2		0.1		0.0		0.1	
7	0.6	0.4			1.7	1.3	**-6.4**			0.6	0.5	0.2	0.9		0.4	0.2			0.2		0.0	0.4		0.4
8								**-0.3**																
9								0.0	**-0.6**					0.1						0.0				
10	0.1	0.0	0.2	0.2					0.1	**-2.3**	0.3		0.3			0.1	0.3	0.2	0.1					
11					0.3	0.3	0.1	0.1		0.2	**-2.7**	0.2	0.0	0.6	0.3	0.1			0.2	0.0	0.0			
12		0.0			0.5	0.1	0.3		0.1		0.6	**-2.2**	0.1	0.2	0.2	0.1				0.0			0.0	
13	0.1	0.0	0.1			0.0	0.2			0.2	0.2		**-1.7**	0.1	0.2	0.1	0.1	0.0						0.1
14		0.0	0.0	0.1		0.1	0.1	0.0	0.1		0.3	0.3	0.0	**-2.4**	0.3	0.1	0.5		0.0			0.0		
15			0.1	0.0	0.1	0.1	0.0	0.0		0.2	0.1	0.2	0.1	0.2	**-2.0**	0.2		0.1		0.0	0.1			0.0
16	0.1			0.1		0.1	0.0			0.1			0.3	0.3	0.1	**-1.9**	0.0	0.1	0.1	0.1	0.0		0.1	0.2
17	0.0		0.3		0.1		0.1		0.2			0.2		0.3	0.4	0.1	**-2.3**	0.2		0.1		0.0		0.2
18	0.1	0.1	0.2		0.1									0.2	0.1	0.1		**-1.0**						0.0
19	0.3	0.0							0.1								0.2	0.1	**-1.0**	0.0		0.0	0.3	
20		0.1																		**-0.3**		0.0		
21						0.1			0.0												**-0.4**			
22																						**-0.4**		
23																							**-0.8**	
24																								**-0.9**

I. As explained in previous sections, these parameter values were obtained by using the historical hourly Ontario energy price (HOEP) data available at [20], and a resulting stochastic model of hourly pricing. This table shows that self elasticities at 2 AM and 7 AM are at least 2 or 3 times higher than the average self-elasticity; additionally, from 3 AM to 6 AM, and then from 10 AM to 5 PM, self elasticities are around the average, while at every other hour these are low. On the other hand, for cross-time elasticities, variations in demand are directly proportional to the variation in prices. Therefore, given the prices, demand is expected to increase at night and decrease during the day.

It is worth mentioning that the higher cross-elasticities are located along the matrix diagonal, meaning that there is a stronger shifting capability between close hours than there is between distant hours. Another interesting observation is that, for the given load EMS, own elasticity values reach values of -8.9, and are higher than 1 for cross elasticity, which means that such EMS technologies are capable of increasing demand elasticity up to 20 times more than the common DR programs, based on the elasticities reported in [5].

C. Benchmark Microgrid Results

In the base case, Fig. 4 displays how the forecasted demand evolves, filling up low demand hours by shifting peaks in demand to the valleys. Since the load model used considers thermal loads, the net value of demand variation is not zero due to thermal inertia, thus increasing demand at the beginning of the 24 hour period and reducing consumption towards the end of the day. This is the same behavior exhibited by the load EMS in [12], where the scheduling is done in a day-ahead basis, resulting in pre-climatizing the building in the morning to meet the constraints during day time.

When comparing Fig. 4 and Fig. 5, one can observe how the demand and prices increase during the night, as expected. It can also be noticed that the morning peak is extended for an hour. Note as well that the total system operating cost for the microgrid decreases as the the demand evolves towards a fixed profile. When considering the operation under stressful conditions, the changes in demand are far more drastic,

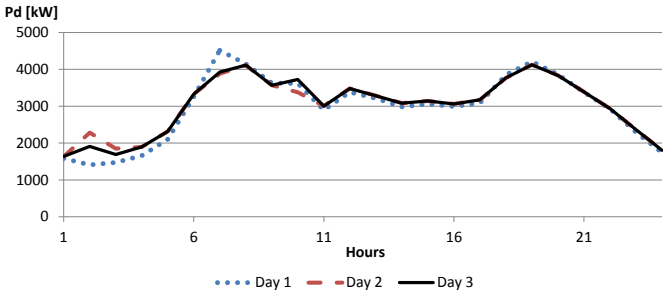

Fig. 4. Effect of DR on total demand for an isolated microgrid.

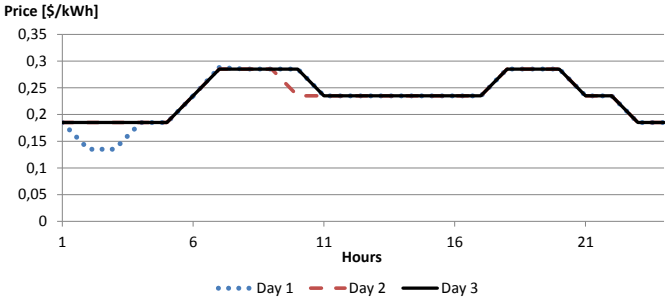

Fig. 5. Effect of DR on pricing signals for an isolated microgrid.

because both the base load and hourly price variability are greater. Figure 6 depicts the evolution of net load in the microgrid showing its convergence to a fixed profile, which is between the initial and first iteration load profiles. This can also be seen in Fig. 7 for price corrections.

Under stressful conditions, the ESS operation occurs more often than for the initial load profile, as shown in Fig. 8. The reason for this is that the system feeders are saturated at the initial loading conditions, and after considering responsiveness, this problem is mostly mitigated. This figure also shows how, after DR activation, the ESS mainly consumes energy from the grid, as to ensure the proper usage of the available energy during periods of high RES generation. It is interesting to note that in the cases presented here, there was no need for DLC usage, as the price-elastic loads and ESS were sufficient to keep the generation-demand balance.

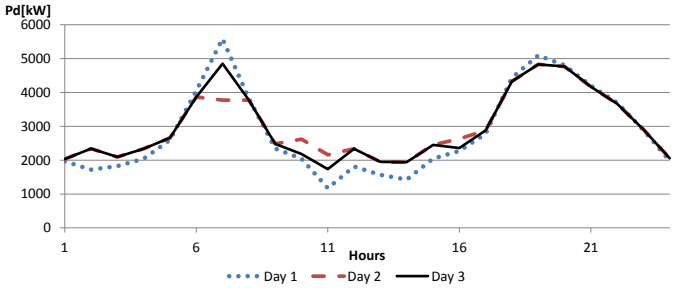

Fig. 6. Effect of DR on total demand for an isolated microgrid under high demand and high content of non-dispatchable RES.

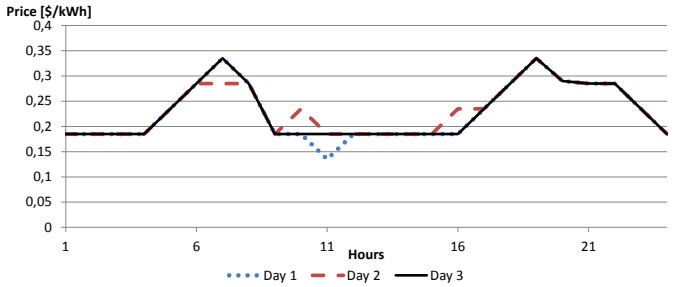

Fig. 7. Effect of DR on pricing signal for an isolated microgrid under high demand and high content of non-dispatchable RES.

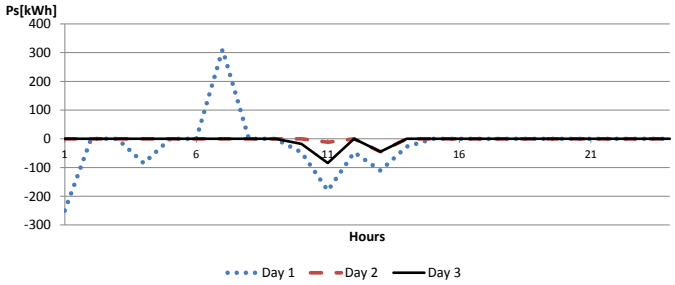

Fig. 8. Effect of DR on ESS operation for an isolated microgrid under high demand and high content of non-dispatchable RES.

V. Conclusions

A new model for studying the effect of load price-elasticity in market prices and dispatch has been developed. It has been shown here, as in previous papers, that price-elastic loads may present adverse effects on the grid, such as the case of low prices, translating into high demand peaks. Hence, DR is demonstrated to not always be as beneficial as some reports claim, especially when elastic demands becomes a significant part of the total system load. Due to the effect of EMS in intelligent loads, demand will be reduced at peak-price, resulting in increase peak power during low-price times, with this phenomenon being more pronounced as the load elasticity increases.

In the particular case of microgrids, multi-period price-responsive loads were shown to have similar behavior as ESS, soothing system variability while minimizing total operating costs. It was demonstrated that there can be a prioritization of DR over ESS, depending on whether the price differences during the day are greater than ESS operating costs or not. However, in the case when there is no other way to meet the demand balance at a certain hour, the prioritization process is nullified.

References

[1] Staff Report, FERC, "Assesment of demand response & advanced metering," http://www.ferc.gov/legal/staff-reports/demand-response.pdf, 2008, [Online].

[2] J. Sheen, C. Chen, and J. Yang, "Time-of-use pricing for load management programs in Taiwan Power Company," *IEEE Transactions on Power Systems*, vol. 9, no. 1, pp. 388–396, 1994.

[3] F. Schweppe, R. Tabors, J. Kirtley, H. Outhred, F. Pickel, and A. Cox, "Homeostatic utility control," *IEEE Transactions on Power Apparatus and Systems*, vol. PAS-99, no. 3, pp. 1151–1163, 1980.

[4] K. Bhattacharya, M. Bollen, and J. Daalder, "Real time optimal interruptible tariff mechanism incorporating utility-customer interactions," *IEEE Transactions on Power Systems*, vol. 15, no. 2, pp. 700–706, 2000.

[5] M. G. Lijesen, "The real-time price elasticity of electricity," *Energy Economics*, vol. 29, no. 2, pp. 249–258, 2007.

[6] R. Yu, W. Yang, and S. Rahardja, "A statistical demand-price model with its application in optimal real-time price," *IEEE Transactions on Smart Grid*, vol. 3, no. 4, pp. 1734–1742, 2012.

[7] O. Corradi, H. Ochsenfeld, H. Madsen, and P. Pinson, "Controlling electricity consumption by forecasting its response to varying prices," *IEEE Transactions on Power Systems*, vol. 28, no. 1, pp. 421–429, 2013.

[8] K. Dietrich, J. Latorre, L. Olmos, and A. Ramos, "Demand response in an isolated system with high wind integration," *IEEE Transactions on Power Systems*, vol. 27, no. 1, pp. 20–29, 2012.

[9] E. Bompard, Y. Ma, R. Napoli, and G. Abrate, "The demand elasticity impacts on the strategic bidding behavior of the electricity producers," *IEEE Transactions on Power Systems*, vol. 22, no. 1, pp. 188–197, 2007.

[10] C. De Jonghe, B. Hobbs, and R. Belmans, "Optimal generation mix with short-term demand response and wind penetration," *IEEE Transactions on Power Systems*, vol. 27, no. 2, pp. 830–839, 2012.

[11] A. Abdollahi, M. Moghaddam, M. Rashidinejad, and M. Sheikh-El-Eslami, "Investigation of economic and environmental-driven demand response measures incorporating UC," *IEEE Transactions on Smart Grid*, vol. 3, no. 1, pp. 12–25, 2012.

[12] M. Bozchalui, S. Hashmi, H. Hassen, C. Cañizares, and K. Bhattacharya, "Optimal operation of residential energy hubs in smart grids," *IEEE Transactions on Smart Grid*, vol. 3, no. 4, pp. 1755–1766, 2012.

[13] M. Carrión and J. Arroyo, "A computationally efficient mixed-integer linear formulation for the thermal unit commitment problem," *IEEE Transactions on Power Systems*, vol. 21, no. 3, pp. 1371–1378, 2006.

[14] A. David, "Load forecasting under spot pricing," *IEE Proceedings C; Generation, Transmission and Distribution*, vol. 135, no. 5, pp. 369–377, 1988.

[15] R. Dufo-López, J. Bernal-Agustín, and J. Contreras, "Optimization of control strategies for stand-alone renewable energy systems with hydrogen storage," *Renewable Energy*, vol. 32, no. 7, pp. 1102–1126, 2007.

[16] E. Castillo, A. J. Conejo, P. Pedregal, R. García, and N. Alguacil, *Building and Solving Mathematical Programming Models in Engineering and Science*. Wiley, 2002.

[17] R. Palma-Behnke, J. Cerda, L. Vargas, and A. Jofre, "A distribution company energy acquisition market model with integration of distributed generation and load curtailment options," *IEEE Transactions on Power Systems*, vol. 20, no. 4, pp. 1718–1727, 2005.

[18] K. Rudion, A. Orths, Z. Styczynski, and K. Strunz, "Design of benchmark of medium voltage distribution network for investigation of DG integration," in *IEEE Power Engineering Society General Meeting*, 2006, pp. 1–6.

[19] K. Divya and J. Østergaard, "Battery energy storage technology for power systems-An overview," *Electric Power Systems Research*, vol. 79, no. 4, pp. 511–520, 2009.

[20] Ontario IESO, "Hourly ontario energy price," http://www.ieso.ca/imoweb/marketdata/hoep.asp, 2012, [Online].